Journal of Photochemistry and Photobiology A: Chemistry 226 (2011) 23–35

Contents lists available at SciVerse ScienceDirect

Journal of Photochemistry and Photobiology A: Chemistry

journal homepage: www.elsevier.com/locate/jphotochem

Formation, photophysical and photochemical properties of water-soluble bismuth(III) porphyrins: The role of the charge and structure

Zsolt Valicsek[a], Ottó Horváth[a,*], Katalin Patonay[a,b]

[a] Department of General and Inorganic Chemistry, Institute of Chemistry, Faculty of Engineering, University of Pannonia, P.O.B. 158, Veszprém H-8201, Hungary
[b] Egerfood Knowledge Center, Eger, H-3300, Leányka u. 6/D, Hungary

ARTICLE INFO

Article history:
Received 29 May 2011
Received in revised form 19 August 2011
Accepted 8 October 2011
Available online 14 October 2011

Keywords:
Water-soluble porphyrin
Out-of-plane
Bismuth(III) ion
Primary photochemistry
Intermediate
S_1- and S_2-fluorescence

ABSTRACT

Bismuth(III) ion forms kinetically labile complexes with the 5,10,15,20-tetrakis(4-sulfonatophenyl)porphyrin anion (H_2TSPP^{4-}) and the 5,10,15,20-tetrakis(1-methyl-4-pyridinium)porphyrin cation (H_2TMPyP^{4+}), the formation constants of which are $3.54 \times 10^4\ M^{-1}$ and $1.62 \times 10^3\ M^{-1}$, respectively (at pH = 6). In these complexes, the metal center, due to its large ionic radius (103 pm), is located out of the ligand plane, distorting it. Accordingly, the absorption and fluorescence spectra of these coordination compounds display special properties characteristic of the so-called sitting-atop (SAT) or out-of-plane (OOP) porphyrin complexes. The shifts of the absorption bands upon metalation indicate that the structural distortion results in stronger perturbation on the S_2- than on the S_1-states of the porphyrin ligand. Metalation significantly decreases the lifetime and the quantum yield of the fluorescence from the S_1 excited state. The relatively rare S_2-fluorescence can also be detected for these metalloporphyrins. Quantum chemical calculations (DFT and TDDFT) confirm the considerable OOP displacement of the Bi(III) center (88 pm) and the typical tendencies of the band-shifts. Differing from the normal (in-plane) metalloporphyrins, excitation of these bismuth(III) porphyrins leads to an irreversible ligand-to-metal charge transfer (LMCT) followed by the opening of the porphyrin ring, which is also typical of SAT complexes. The quantum yields of this photoinduced redox reaction are significantly higher for the anionic than for the cationic complex, due to the stronger Lewis-basicity of H_2TSPP^{4-}. In the mechanism of the reaction between these free-base porphyrins and bismuth(III) ions formation of a longer-lived intermediate was observed. In the case of the cationic porphyrin also the photochemistry of this intermediate could be studied; deviating from the photoinduced behavior of the final product metalloporphyrins, excitation of this intermediate results in predominantly the dissociation to the initial porphyrin ligand and metal ion, indicating a relatively weak coordination bond and significantly distorted structure.

1. Introduction

Metalloporphyrins play key roles in several biochemical processes, such as photosynthesis and oxygen transport as well as in various redox reactions [1–8]. Within this important group of compounds the so-called out-of-plane (OOP) or sitting-atop (SAT) metalloporphyrins are characterized by special properties [9–12] originating from the non-planar structure caused by, first of all, the size of the metal center. In these complexes, the ionic radius (>80–90 pm) of the metal center is too large to fit into the cavity of the ligand, hence it is located above the porphyrin plane, distorting it. The symmetry of this structure is lower (generally C_{4v}–C_1) than that of both the free-base porphyrin (D_{2h}) and the regular, coplanar metalloporphyrins (D_{4h}), in which the metal center fits into the ligand cavity. The rate of formation of in-plane (or normal) metalloporphyrins is much slower than that of the OOP complexes because of the rigidity of porphyrins. Larger metal ions such as Pb^{2+}, Hg^{2+}, or Cd^{2+}, however, can catalyse the formation of normal metalloporphyrins via generation of OOP complex intermediates [13–18]. In these species the distortion caused by the out-of-plane location of the larger metal center makes two diagonal pyrrolic nitrogens more accessible to another metal ion, even with smaller ionic radius, on the other side of the porphyrin ligand [19].

Deviating from the normal (coplanar) metalloporphyrins, the SAT complexes, on account of their distorted structure and kinetic lability, display special photochemical properties, such as photoinduced charge transfer from the porphyrin ligand to the metal center, leading to irreversible ring opening of the ligand and dissociation on excitation at both the Soret- and the Q-bands [20]. The absorption and emission features of these complexes also significantly differ from those of the in-plane metalloporphyrins.

* Corresponding author. Tel.: +36 88 624 159; fax: +36 88 624 548.
E-mail addresses: valicsek@vegic.uni-pannon.hu (Z. Valicsek), otto@vegic.uni-pannon.hu (O. Horváth), pkata15@gmail.com (K. Patonay).

1010-6030/$ – see front matter © 2011 Elsevier B.V. All rights reserved.
doi:10.1016/j.jphotochem.2011.10.011

The photoinduced behavior of normal metalloporphyrins have been thoroughly studied for several decades, while the investigation of OOP complexes started in this respect only in the past 8–10 years. The size of bismuth(III) with an ionic radius of 103 pm [21] is favorable for the formation of OOP metalloporphyrins. Accordingly, several studies have been published regarding such complexes of bismuth(III) with various hydrophobic porphyrins. The 1:1 complexes with simple porphyrin ligands (such as octaethyl or tetratolyl porphyrins) proved to be kinetically labile [22–29], similarly to the corresponding dimers in which the monomers are connected with two axially coordinated halogen bridges [25]. Thus, for medical applications in radio-immunotherapy, Boitrel and coworkers prepared special porphyrin derivatives functionalized with pendant arms (pickets) terminated with various groups of oxygen donor atoms [26,30–33] or with a strap with a hanging carboxylate group [34–36] in order to hinder the demetalization of these metalloporphyrins. The main Soret-band of the hydrophobic bismuth(III) porphyrins display a strong red shift compared to that of the corresponding free base. Its wavelength is in the range of 457–479 nm, depending on the substituents of the porphyrin ring and the axial ligands. The out-of-plane displacement of the metal center in the crystal structure was found to be 107–131 pm, the larger distances in this range belong to complexes with various axial ligands [24–26,30,31,36]. These values are in accordance with those determined for bismuth(III) phthalocyanines (112–115 pm [37], 149 pm [38]).

These types of metalloporphyrins displaying such a large red shift were called hyperporphyrins by Gouterman [24], especially if the metal ion is a *p*-field element then *p*-type hyperporphyrins. Gouterman's definition was applied for the complexes the electronic spectrum of which in the visible region could not be described by his 4 MO-model [39]. Since specially substituted free-base porphyrins (such as protonated meso-(dimethylaminophenyl)porphyrins) display similar spectral phenomena, his interpretation had to be modified [40]. Eventually, the request for the re-interpretation of hyperporphyrins was born on the basis of the highly distorted structure of these porphyrins showing strong red shifts [41].

Probably due to the difficulty caused by the strong inclination of Bi^{3+} to hydrolyse, the only water-soluble bismuth(III) porphyrin has been prepared so far with 5,10,15,20-tetrakis(1-methyl-4-pyridinium)porphyrin; the complex displayed a 465-nm Soret-band [42], which also suggests a significant OOP displacement. In spite of the numerous papers on bismuth(III) porphyrins, photochemical features of these complexes have not been investigated yet, neither in organic nor in aqueous systems. Only a hydrophobic tetrapyrrole complex of bismuth(III), with the porphyrin-like triphenyl corrole, was studied quite recently in structural and photochemical points of view [43]. Its irradiation led to the oxidation of the metal center.

On the basis of the precedents in this topic, the aim of our work, in the frame of a systematic investigation of the photophysics and photochemistry of water-soluble, sitting-atop metalloporphyrins, was to study the formation and mainly the photoinduced behavior of the bismuth(III) complexes with 5,10,15,20-tetrakis(4-sulfonatophenyl)porphyrin and 5,10,15,20-tetrakis(1-methyl-4-pyridinium)porphyrin, an anionic and a cationic ligand (Fig. 1). The effects of the charge and the molecular structure on the formation, photophysical and photochemical properties were also examined in this work.

2. Experimental

2.1. Reagents and solutions

Analytical grade tetrasodium 5,10,15,20-tetrakis(4-sulfonatophenyl)porphyrin ($Na_4H_2TSPP{\cdot}12H_2O$), 5,10,15,20-tetrakis(1-methyl-4-pyridinium)porphyrin tetra(p-toluenesulfonate) (H_2TMPyP tetratosylate salt) and $Bi(NO_3)_3{\cdot}5H_2O$ (Sigma–Aldrich) were used for the experiments. The solvent was double-distilled water purified with Millipore Milli-Q system. Oxygen-free experiments were carried out by argon-bubbling and the Schlenk technique prior to the irradiation. The solutions containing metalloporphyrin were prepared well (at least 1 day) before the photophysical and photochemical experiments so that the onset of complex equilibration was ensured. The actual concentrations of the porphyrin stock solutions prepared were checked spectrophotometrically, using the molar absorptions of the reagents at characteristic wavelengths. The pH of each solution was adjusted to 6 by application of acetate buffer, also keeping the ionic strength at constant value of 1 M. It is worth mentioning that the acetate buffer was utilized also to avoid hydrolysis of Bi(III) ions. Too low a pH could not be applied because H_2TSPP^{4-} is protonated at pH = 5 ($pK_3 = 4.99$, $pK_4 = 4.76$ [44]). Since bismuth(III) ions are strongly prone to hydrolysis, a rather high concentration of buffer was used (1 M).

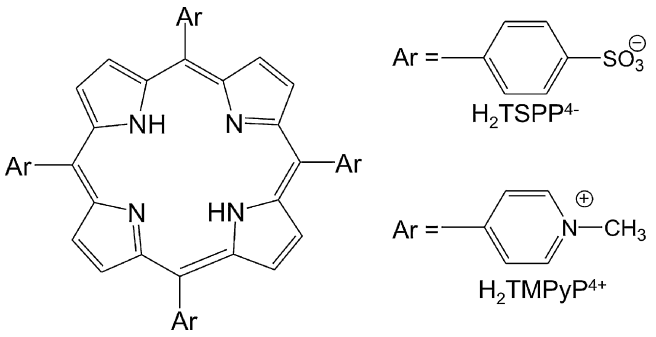

Fig. 1. Structures of 5,10,15,20-tetrakis(4-sulfonatophenyl)porphyrin (H_2TSPP^{4-}) and 5,10,15,20-tetrakis(1-methyl-4-pyridinium)porphyrin (H_2TMPyP^{4+}).

2.2. Instruments and procedures

The absorption spectra were recorded and the photometric titrations were monitored using a Specord S-100 and a Specord S-600 diode array spectrophotometer. For the measurement of fluorescence spectra a Perkin ELMER LS 50-B and a Horiba JobinYvon Fluoromax-4 spectrofluorimeter were applied. The latter equipment supplemented with a time-correlated single-photon counting (TCSPC) accessory was utilized for determination of fluorescence lifetimes, too. Rhodamine-B and $Ru(bpy)_3Cl_2$ were used as references for correction of the detector sensitivity and for determination of the fluorescence quantum yields [45,46]. Each compound studied was excited at the wavelength of its absorption maximum. Luminescence spectra were corrected for detector sensitivity. For the elimination of the potential reabsorption effects in the detection of luminescence low concentration and a holder for solid samples were applied. In this case, the emitted light beam arrives from the surface of the cell to the detector. Moreover, because of the small Stokes-shifts and the disturbing effect of the (Rayleigh and) Raman scattering, the spectrum analyses were carefully carried out by fitting Gaussian and Lorentzian curves in MS Excel.

For continuous irradiations an AMKO LTI photolysis equipment (containing a 200-W Xe–Hg-lamp and a monochromator) was applied [47]. Incident light intensity was determined with a thermopile calibrated by ferrioxalate actinometry [48,49]. Quartz cuvettes of 1 and 5 cm pathlength were utilized as reaction vessels. During the irradiations the reaction mixtures were continuously homogenized by magnetic stirring. All measurements were carried out at room-temperature. The experimental results were processed and evaluated by MS Excel programs on PCs.

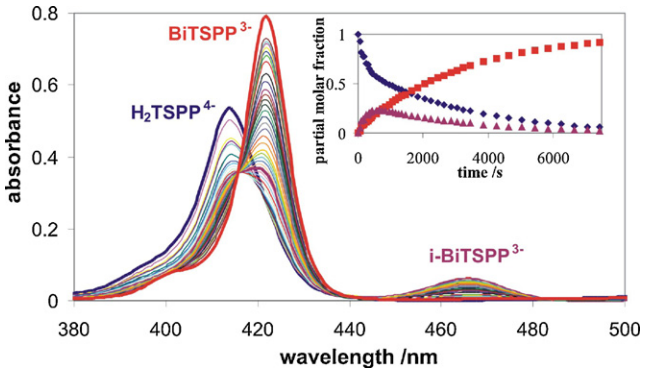

Fig. 2. Spectral changes during the reaction of 1.08×10^{-6} M H_2TSPP^{4-} and 3.00×10^{-4} M Bi^{3+} in the presence of 1 M acetate buffer (pH ≈ 6, l = 1 cm). Insert: partial molar fractions vs. time plots for the free base (H_2TSPP^{4-}, ◆), the intermediate (i-$BiTSPP^{3-}$, ▲), and the final complex ($BiTSPP^{3-}$, ■).

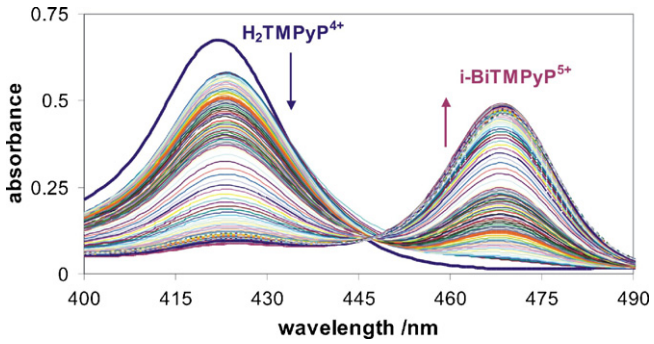

Fig. 3. Spectral changes during the reaction of 2.97×10^{-6} M H_2TMPyP^{4+} and 3.36×10^{-4} M Bi^{3+} in the presence of 0.01 M acetate buffer (pH ≈ 4, l = 1 cm, Δt = 1 s).

2.3. Electronic structure calculations

Electronic structure calculations involved molecular geometry optimization and the determination of vertical electron excitation energies. For both purposes we applied density functional theory, in particular, the B3LYP combination of functionals [50–52], and time-dependent density functional. In the geometry optimizations we used the Hay-Wadt valence double-zeta (LANL2DZ) basis set [53–55] in which the influence of the inner-shell electrons on the valence shell is described using effective core potentials (ECP) for Bi. During our previous tests we found that the sulfonato-phenyl substituent has a negligible effect on the coordination site, thus in the present calculations we modeled H_2TSPP^{4-} and H_2TMPyP^{4+} with unsubstituted porphin, H_2P. All calculations were performed using the Gaussian 03 suite of programs [56].

3. Results and discussion

3.1. Formation and absorption spectra

Kinetically labile complexes are mostly examined in the excess of the ligand. In the case of metalloporphyrins, however, metal ions are applied generally in excess, especially for spectrophotometric measurements, partly because of the extremely high molar absorbances (mainly at the Soret-bands) of the porphyrins. The formation of kinetically labile OOP complexes, deviating from the coplanar (normal) metalloporphyrins, is an equilibrium process. It can be spectrophotometrically monitored because the absorption and emission bands assigned to ligand-centered electron transitions undergo significant shift and intensity change upon coordination of metal ions.

As Fig. 2 displays in the case of the anionic porphyrin, in the reaction of the bismuth(III) ion with the free-base porphyrin the formation of an intermediate can be observed. Disappearance of the characteristic Soret-band of H_2TSPP^{4-} at 413 nm is accompanied by the temporary appearance of a new band at 465 nm. The decay of this intermediate leads to the formation of the final complex, indicated by the gradual increase of the band at 421 nm. This wavelength fully agrees with that of the Soret-band of the corresponding 1:1 complexes with Hg(II), Hg(I), Tl(III), Fe(II) and Cd(II) ions [57–63], suggesting that, similarly to these metalloporphyrins, an OOP or SAT complex was formed. As the insert in Fig. 2 shows, the decay of the intermediate in the case of the anionic porphyrin is rather fast, thus the formation of the final complex took place from the beginning of the reaction.

In the case of the cationic porphyrin the decay of the intermediate, i.e., the formation of the final complex is much slower than for the anionic complex, probably as a consequence of the positive charge on the ligand repulsing the metal ions. Besides, the lower Lewis-basicity of the cationic porphyrin diminishes the driving force of the coordination. Since, for the same reason, the protonation constants of H_2TMPyP^{4+} (pK_3 = 1.8, pK_4 = 0.7 [64]) are much lower than those of H_2TSPP^{4-}, a lower pH can also be used in this system. Thus, decreasing the concentration of the buffer and keeping the concentration of bismuth(III) constant (3×10^{-4} M), pH was decreased to 4, which was favorable for the accumulation of the intermediate. Hence, accumulation of the intermediate can be reached in this case as it is demonstrated in Fig. 3. Under these circumstances the lifetime of the intermediate formed was about 2 h, during which its photophysical and photochemical properties could also be studied. It is worth mentioning that the absorption spectrum of the intermediate with both anionic and cationic ligands is very similar to those of the hydrophobic metalloporphyrins published. The large red shift of the Soret-band is indicative of a significantly distorted structure caused by the considerable out-of-place displacement of the metal center. A similar absorption spectrum was observed for the bismuth(III) complex with the cationic porphyrin [42], indicating that under the circumstances applied in that work such an intermediate-type species was formed (but this type does not originate from the pyrrol-protons in water, rather probably from the potential axial ligands, as OH^- or Ac^-, which may dissociate to give the end-product complex).

The formation and disappearance of the intermediate observed with both porphyrins applied in this study can be taken into account by Eqs. (1) and (2), where H_2P is the abbreviation for the free-base porphyrin, i-$Bi^{III}P$ for the intermediate, and $Bi^{III}P$ for the final, end-product complex (the charges are omitted).

$$Bi^{3+} + H_2P \Leftrightarrow \text{i-}Bi^{III}P + 2H^+ \quad (1)$$

$$\text{i-}Bi^{III}P \Leftrightarrow Bi^{III}P \quad (2)$$

Eq. (3) describes the overall equilibrium for the formation of the final complex, no matter if it is formed directly or via intermediate.

$$Bi^{3+} + H_2P \Leftrightarrow Bi^{III}P + 2H^+ \quad (3)$$

The overall formation constant (K) can be written for this equilibrium. However, we have determined the apparent stability constant (K') because the measurements were carried out at an unvaried pH of 6 (Eqs. (4)–(6)).

$$K' = \frac{K}{[H^+]^2} = \frac{[Bi^{III}P]}{[Bi^{3+}][H_2P]} \quad (4)$$

$$\phi_1 = \frac{[Bi^{III}P]}{[H_2P] + [Bi^{III}P]} = \frac{K'[Bi^{3+}]}{1 + K'[Bi^{3+}]} \quad (5)$$

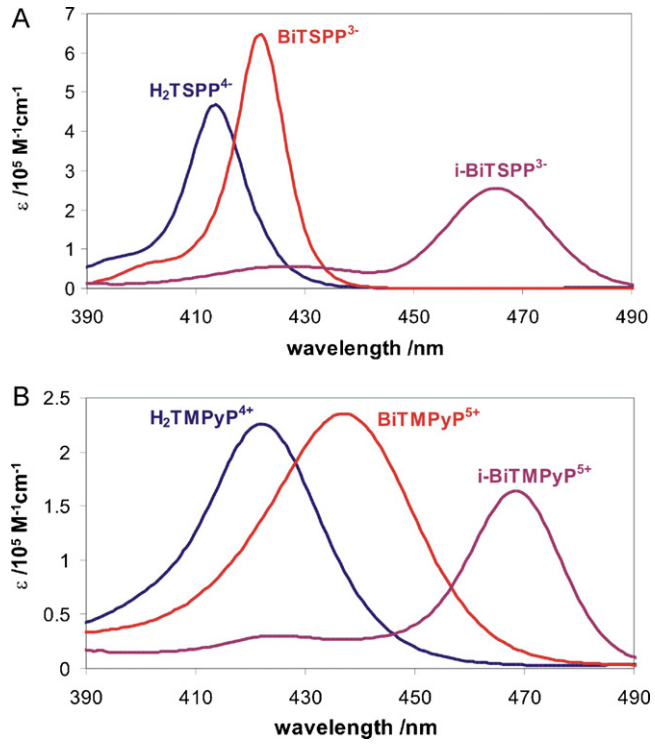

Fig. 4. Molar absorption spectra of the anionic (A) and cationic (B) metalloporphyrins ($BiTSPP^{3-}$ and $BiTMPyP^{5+}$), intermediates (i-$BiTSPP^{3-}$ and i-$BiTMPyP^{5+}$), and the corresponding free-bases (H_2TSPP^{4-} and H_2TMPyP^{4+}) in the range of the Soret-bands.

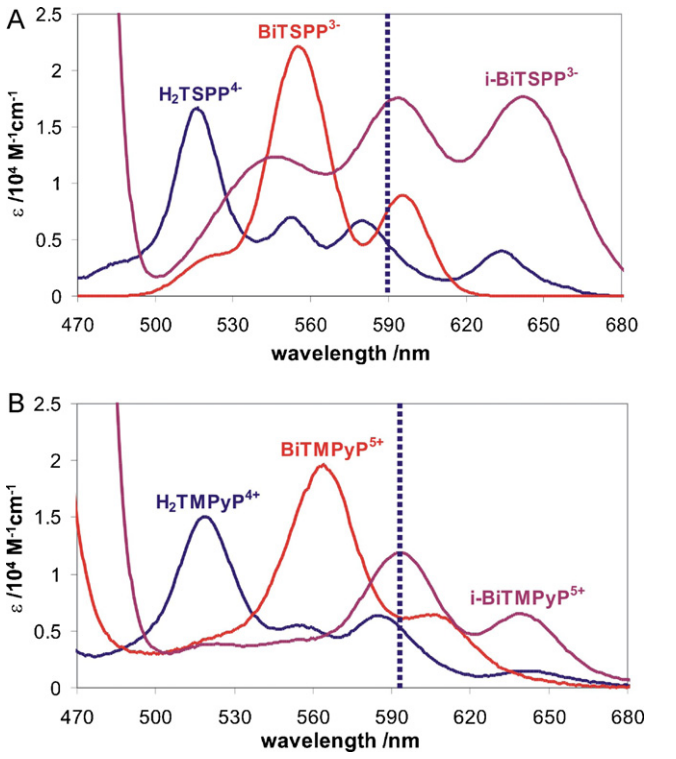

Fig. 5. Molar absorption spectra of the anionic (A) and cationic (B) metalloporphyrins ($BiTSPP^{3-}$ and $BiTMPyP^{5+}$), intermediates (i-$BiTSPP^{3-}$ and i-$BiTMPyP^{5+}$), and the corresponding free-bases (H_2TSPP^{4-} and H_2TMPyP^{4+}) in the range of the Q-bands. The dotted lines represent the average energy $Q_y(0,0)$ and $Q_x(0,0)$ of free-base porphyrins.

$$\phi_0\varepsilon_{H_2P,\lambda} + \phi_1\varepsilon_{Bi^{III}P,\lambda} = \frac{\varepsilon_{H_2P,\lambda} + K'[Bi^{3+}]\varepsilon_{Bi^{III}P,\lambda}}{1 + K'[Bi^{3+}]} \quad (6)$$

ϕ_0 and ϕ_1 are the partial molar fractions of the different porphyrin forms {0 = free-base, 1 = complex}, $\varepsilon_{i,\lambda}$ is the corresponding molar absorbance at λ wavelength. Eq. (6) expresses the average molar absorbance of the porphyrin species (free-base and complexed). During the evaluation of the average molar absorbance vs. $[Bi^{3+}]$ data, an iterative least-square procedure (based on Eq. (6)) was used to find the best fitting values of K' and $\varepsilon(Bi^{III}P, \lambda)$ parameters. Due to the significant band-shifts, as a consequence of the strong coordination bond, absorbances in the range of both Soret- and Q-bands were used for such an evaluation giving $K' = 3.54 \times 10^4\ M^{-1}$ for $BiTSPP^{3-}$ and $1.62 \times 10^3\ M^{-1}$ for $BiTMPyP^{5+}$ at pH = 6. The formation constant for the anionic complex is more than one order of magnitude higher than that for the cationic complex, indicating that the negative charge (−4) enhances the Lewis-basicity of the porphyrin ligand, resulting in a more stable coordination compound than in the case of the positively charged ligand of reduced basicity. The absolute values of the equilibrium constants indicate that the thermodynamic stability of these complexes is not really high. Compared the value of K' for $BiTSPP^{3-}$ to that for the corresponding complex of mercury(II), $HgTSPP^{4-}$ ($K' = 8.82 \times 10^5\ M^{-1}$ [57]), the latter is one order of magnitude higher, although the ionic radius of Hg^{2+} is 103 pm [21], i.e., about the same as that of Bi^{3+}. In this case the difference may be attributed to the softer Pearson-acidity of the mercury(II) ion better fitting to the also softer pyrrol-nitrogens.

The molar absorption spectra of the anionic and cationic porphyrins (the intermediate, the final metalloporphyrins, and the corresponding free bases) are displayed in Figs. 4 and 5 for the Soret- and Q-bands, respectively. The corresponding characteristic absorption data are summarized in Tables 1 and 2.

The band-shifts refer to the Soret- or B(0,0) and the Q(0,0) transitions, where the first number in parentheses indicates the vibrational quantum number of the excited (the S_2 and S_1 states, respectively), the second that of the ground electronic state [65,66]. The determination of the magnitude of the red shift is complicated because the presence of pyrrol-hydrogens in free-base porphyrin reduces the symmetry ($D_{4h} \rightarrow D_{2h}$) and splits the Q-band ($Q \rightarrow Q_x + Q_y$) [67], hence there are generally five bands in this spectral region of free-base-, in contrast to three in those of metalloporphyrins [68] (Table 2). According to Gouterman's suggestion [39], the shift was calculated with respect to the average energy of the $Q_x(0,0)$ and $Q_y(0,0)$ bands of the free-base porphyrin.

As a consequence of the coordination of bismuth(III) ion, both the Soret-bands (at 350–500 nm) and the Q-bands (at 500–700 nm) are red-shifted in the case of both water-soluble porphyrins. The molar absorbances of the main Soret- and Q-bands of the metalloporphyrins (B(0,0) and Q(1,0)) are higher than the corresponding values for the free-base porphyrin. According to our earlier observations [20,57,58,60–63,69] this type of spectral features is unambiguously characteristic for OOP or SAT complexes, confirming the expectations based on the size (103 pm ionic radius) of Bi(III). The absolute values of the molar absorbances are higher for the anionic porphyrins than for the corresponding cationic ones in the cases of the free-base as well as the metalloporphyrins.

Besides, the difference of both the charge and the structure between the two ionic porphyrins results in significant red shifts of the main bands in the case of H_2TMPyP^{4+} compared to those of H_2TSPP^{4-}. These red shifts can also be observed in the comparison of the anionic and cationic metalloporphyrins too (Tables 1 and 2). The red shift of absorption in heavy-metal porphyrins can be attributed to that the metal orbitals are closer in energy to the antibonding π^* molecular orbitals (lowest unoccupied molecular

Table 1
Characteristic data of the absorption spectra of the anionic (A) and cationic (B) metalloporphyrins ($BiTSPP^{3-}$ and $BiTMPyP^{5+}$), intermediates (i-$BiTSPP^{3-}$ and i-$BiTMPyP^{5+}$), and the corresponding free-bases (H_2TSPP^{4-} and H_2TMPyP^{4+}) in the range of the Soret-bands.[a]

Species	H_2TSPP^{4-} [b]	$BiTSPP^{3-}$	i-$BiTSPP^{3-}$	H_2TMPyP^{4+}	$BiTMPyP^{5+}$	i-$BiTMPyP^{5+}$
λ {B(1,0)}/nm	395	405	426	395	400	426
ε_{max} {B(1,0)}/10^4 M^{-1} cm^{-1}	8.09	7.26	6.12	5.33	4.14	3.01
λ_{Gauss}{B(1,0)}/nm	396	407	427	397	404	431
ε_{Gauss}{B(1,0)}/10^4 M^{-1} cm^{-1}	8.13	8.69	5.57	5.30	4.07	2.94
$\omega_{1/2}${B(1,0)}/cm^{-1}	1149	1063	1854	1582	2117	2004
f{B(1,0)}	0.361	0.357	0.399	0.324	0.333	0.228
ν{B(1,0)}/cm^{-1}	1090	875	1915	1539	1841	1839
λ{B(0,0)}/nm	413	421	466	422	437	468
ε_{max}{B(0,0)}/10^5 M^{-1} cm^{-1}	4.66	6.44	2.63	2.26	2.35	1.64
λ_{Gauss}{B(0,0)}/nm	414	422	465	422	437	468
ε_{Gauss}{B(0,0)}/10^5 $M^{-1'}$ cm^{-1}	4.45	6.18	2.52	2.20	2.28	1.59
$\omega_{1/2}${B(0,0)}/cm^{-1}	785	625	997	1380	1629	974
f{B(0,0)}	1.35	1.49	0.971	1.17	1.44	0.598
B-shift (metalation)/cm^{-1}	–	−457	−2669	–	−766	−2296
B-shift (substitution)/cm^{-1}	–	–	–	−492	−800	−119

[a] λ, measured wavelength; λ_{Gauss}, wavelength from spectrum analysis; $\omega_{1/2}$, halfwidth; f, oscillator strength; ν, energy of vibronic origin or overtone.
[b] From Ref. [53].

orbitals, LUMOs) than to the binding π orbitals (highest occupied molecular orbital, HOMO) of porphyrin, so that the perturbation they cause decreases the energy of the LUMOs more than that of the HOMO, resulting in the bathochromic effect of $\pi\pi^*$ transitions. Besides, the structural change of the macrocyclic ligand, due to the interaction with the metal center of large ionic radius, may also contribute to this spectral property. Regarding the final complexes, metalation of the cationic porphyrin causes larger red shifts than that of the anionic porphyrin, indicating a more significant structural change and electronic perturbation in the previous case.

The main bands of the intermediate metalloporphyrins (i-$BiTSPP^{3-}$ and i-$BiTMPyP^{5+}$) display very strong red shifts compared even to those of the corresponding end-product metalloporphyrins ($BiTSPP^{3-}$ and $BiTMPyP^{5+}$, respectively). These dramatic shifts can be attributed to a considerable distortion of the porphyrin plane, a much more significant than that in the final complexes. This suggests that in the intermediates the metal center is located at larger distance out of the ligand plane, resulting in a higher dome-distortion (and probably a superposing ruffled-distortion similarly to lead(II)-porphyrins [10]) of the ligand. Interestingly, the wavelengths of the main Soret- and Q-bands of the cationic intermediate hardly differ from those of the anionic one, deviating from the observation in the case of the end-product metalloporphyrins. This phenomenon suggests that for the intermediate complexes the energies of the electronic transitions are determined by rather the metal–ligand interaction than the effects of the ionic substituents, i.e., the electronic and mainly the steric, distorting effect of the bismuth(III) center is the predominant factor in this respect. This conclusion is in accordance with the observation that the absorption spectrum of the hydrophobic bismuth(III) porphyrins [25–36] are very similar to those of the water-soluble intermediate complexes. Apparently, in hydrophobic systems these types of

Table 2
Characteristic data of the absorption spectra of the anionic (A) and cationic (B) metalloporphyrins ($BiTSPP^{3-}$ and $BiTMPyP^{5+}$), intermediates (i-$BiTSPP^{3-}$ and i-$BiTMPyP^{5+}$), and the corresponding free-bases (H_2TSPP^{4-} and H_2TMPyP^{4+}) in the range of the Q-bands (for notations see Table 1).

Species	H_2TSPP^{4-} y[b]	H_2TSPP^{4-} x[b]	$BiTSPP^{3-}$	i-$BiTSPP^{3-}$	H_2TMPyP^{4+} y	H_2TMPyP^{4+} x	$BiTMPyP^{5+}$	i- $BiTMPyP^{5+}$
λ{Q(2,0)}/nm	490		519	562	490		520	555
ε_{max}{Q(2,0)}/$M^{-1}cm^{-1}$	3347		3236	7197	3720		4312	4258
λ_{Gauss}{Q(2,0)}/nm	489		522	546	488		520	555
ε_{Gauss}{Q(2,0)}/$M^{-1}cm^{-1}$	3167		3419	12,300	3486		4483	3717
$\omega_{1/2}${Q(2,0)}/cm^{-1}	1121		1000	1840	1080		1552	1321
f{Q(2,0)}	0.0137		0.0255	0.0875	0.0145		0.0269	0.019
ν{Q(2,0)}/cm^{-1}	1080		1145	1517	1205		1458	1179
λ{Q(1,0)}/nm	516	579	556	595	519	586	564	594
ε_{max}{Q(1,0)}/$M^{-1}cm^{-1}$	16,657	6669	22,928	17,209	15,012	6337	19,615	11,906
λ_{Gauss}{Q(1,0)}/nm	517	582	555	595	519	586	563	594
ε_{Gauss}{Q(1,0)}/$M^{-1}cm^{-1}$	16,062	6155	22,031	15,368	14,799	6026	18,804	11,522
$\omega_{1/2}${Q(1,0)}/cm^{-1}	827	846	861	1027	1016	949	1060	958
f{Q(1,0)}	0.0513	0.0201	0.0733	0.061	0.0581	0.0221	0.0771	0.0427
ν{Q(1,0)}/cm^{-1}	1180	1385	1219	1246	1197	1466	1458	1179
λ{Q(0,0)}/nm	553	633	596	643	556	644	608	639
ε_{max}{Q(0,0)}/$M^{-1}cm^{-1}$	6985	3980	9008	18,075	5507	1483	6400	6496
λ_{Gauss}{Q(0,0)}/nm	550	633	596	643	553	642	607	640
ε_{Gauss}{Q(0,0)}/$M^{-1}cm^{-1}$	6433	3676	8887	17,369	4949	1405	6027	6291
$\omega_{1/2}${Q(0,0)}/cm^{-1}	830	727	628	1019	866	961	922	848
f{Q(0,0)}	0.0206	0.0103	0.0216	0.0684	0.0166	0.0052	0.0215	0.0206
B–Q energy gap/cm^{-1}	7174		6920	5939	6841		6438	5752
Q-shift (metalation)/cm^{-1} [a]	–	–	−203	−1434	–	–	−362	−1207
Q-shift (substitution)/cm^{-1}	–	–	–	–	−103	−213	−317	68
$\varepsilon(B_{max})/\varepsilon(Q_{max})$	28		28.1	14.5	15.1		12	13.8
f(B)/f(Q)	14.7		15.4	6.3	12.9		14.1	10

[a] Compared to the average of the free-base's $Q_y(0,0)$ and $Q_x(0,0)$ bands.
[b] From Ref. [53].

metalloporphyrins are the end-products of metalation of free-base porphyrins. This phenomenon may be attributed to the appreciable coordination ability or the polarizing effect of water molecules, which can promote the complex to overcome the kinetic energy barrier toward the more stable structure, in which the metal center is located closer to the ligand plane. Notably, not only the significant red shift of the main Soret- and Q-bands are characteristic of these intermediates, but their molar absorbances too, which are considerably lower even than those of the corresponding free-base porphyrins (Tables 1 and 2). This may be also the consequence of the strongly distorted structure.

As a consequence of intensity borrowing, the vibrational fine structure, the transitions to higher vibrational levels of the excited electronic states also appear in the electronic spectra of porphyrins [70,71]. The frequencies of the vibronic origins {B(1,0) and Q(1,0) bands }and their potential overtones {Q(2,0)} for the porphyrins studied in this work (ν in Tables 1 and 2) were determined by spectrum analysis (more accurately than taken directly from the measured spectra). The tendecies of the frequencies of the vibronic origins, overtones obtained for the free-base-, the intermediate, and the final metalloporphyrins are the same as those observed for the main bands (B(0,0) and Q(0,0)). The energy gap between the B(0,0)- and Q(0,0)-bands decreases upon metalation, moderately for the final and more significantly for the intermediate metalloporphyrins for both the anionic and the cationic complexes (Tables 1 and 2). This tendency indicates that the structural distortion results in stronger perturbation on the S_2- than on the S_1-states of the porphyrin ligand. This effect is clearly manifested in the values of f(B)/f(Q) ratios for the intermediate complexes (Table 2).

3.2. Emission

Both the anionic and the cationic complexes of bismuth(III) display appreciable fluorescence upon excitation at the Soret- or the Q-bands. The fluorescence spectra of $BiTSPP^{3-}$ and $BiTMPyP^{5+}$ are compared to those of the corresponding free-base porphyrin in Fig. 6. The characteristic data for the S_1-fluorescence of the metalloporphyrins studied and those of the corresponding free bases are summarized in Table 3.

Fig. 6 shows, coordination of the metal ion to the porphyrin ligand results in a strong blue shift of the emission bands and a significant decrease of the fluorescence intensity (i.e. quantum yield).

The hypsochromic effect in the fluorescence, i.e., the shift of the (0,0) band (by 500–1000 cm^{-1}, Table 3), is in contrast with the red shift in the absorption. Notably, this blue shift–red shift anomaly is virtual, because the absorption shift is referred to the average of Q_y(0,0)- and Q_x(0,0)-bands of the free-base ligand, while the emission derives not from a hypothetical average level, but from the energetically lower S_{1x}-state (populated in Q_x(0,0) absorption) [63].

Both phenomena suggest that the structure of the originally flat (free-base) ligand is distorted in these metalloporphyrins. The reduction of the quantum yield is especially conspicuous in the case of the anionic complex (from 0.075 to 0.019), which can be attributed to the stronger interaction between the ligand and the metal center, due to the higher Lewis-basicity of H_2TSPP^{4-} compared to that of H_2TMPyP^{4+}. Nevertheless, metalation significantly diminishes the quantum yield also in the case of the cationic porphyrin (from 0.030 to 0.019).

Similar tendencies of the band-shifts and quantum yields were observed in the fluorescence of typical OOP metalloporphyrins such as $Hg(II)TSPP^{4-}$, $(Hg(I)_2)_2TSPP^{2-}$, $Cd(II)TSPP^{4-}$, $Tl(I)_2TSPP^{4-}$ or $Fe(II)TSPP^{4-}$ [57–63,69]. This feature, in accordance with the characteristics of the absorption spectra, confirms that $BiTSPP^{3-}$ and $BiTMPyP^{3+}$ are of sitting-atop or out-of-plane type. Notably, this is the first case that typical SAT fluorescence was observed for a cationic metalloporphyrin. In order to prove that both the Soret- and the Q-band excitation leads to the fluorescence, the excitation spectra of the metalloporphyrins studied were also determined. The monitoring wavelength was that of the longer-wavelength band at each complex. The spectra obtained (Fig. S1) exactly agree with the corresponding absorption spectra, clearly indicating that these emissions unambiguously originate from the excited states of these metalloporphyrins.

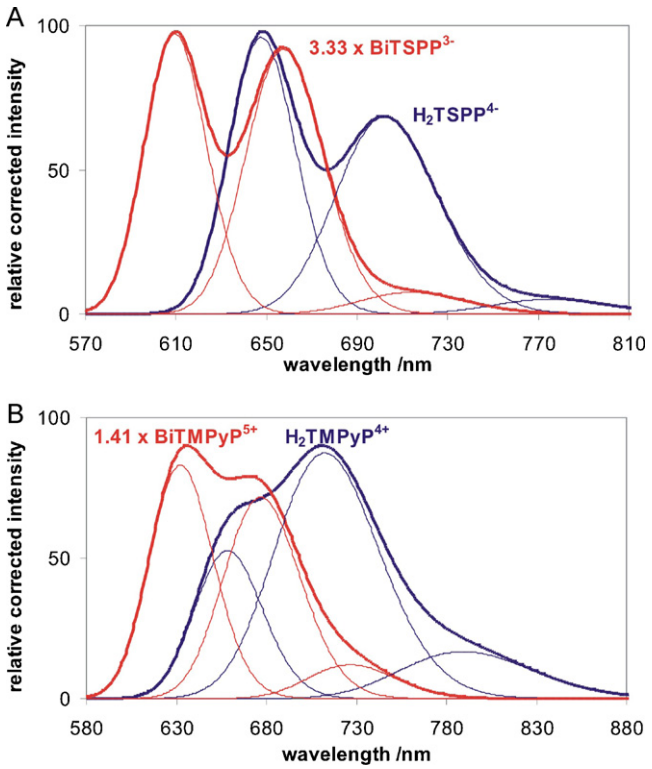

Fig. 6. S_1-fluorescence spectra of the anionic (A) and cationic (B) metalloporphyrins ($BiTSPP^{3-}$ and $BiTMPyP^{5+}$) compared to the corresponding free-bases (H_2TSPP^{4-} and H_2TMPyP^{4+}) upon excitation at their absorption maxima or the isosbestic point in the titrations spectral series, respectively.

Metalation of the anionic porphyrin slightly increases the S_1-Stokes-shift (360 cm^{-1} vs. 376 cm^{-1}), similarly to the corresponding complexes of mercury(II) and cadmium(II) [58,63], while for the cationic porphyrin a significant enhancement (from 398 cm^{-1} to 651 cm^{-1}) can be observed, indicating that the geometrical change (nonplanar distortion) between the ground and the S_1-excited states considerably increases in the latter case. Accordingly, the blue shift of the S_1(0,0) emission band upon metalation is much larger for the anionic than for the cationic porphyrins (941 cm^{-1} vs. 534 cm^{-1}), while the red shifts of the corresponding absorption bands display the opposite tendency (Table 2).

Since excitation at both the Soret- and the Q-bands leads to the same emission spectrum in the 550–800-nm range, the fluorescence takes place from the same excited state (S_1), i.e., excitation to the S_2 state is followed by an efficient internal conversion to the S_1 state. The efficiency of the IC can be determined from the fluorescence quantum yields measured at the Soret- and the Q-bands (Table 3). The values of Φ_{IC} are about 0.7–0.8, metalation causes a moderate decrease for the anionic, while an increase for the cationic porphyrin. The significant decrease of the quantum yield and the S_1 excited-state lifetime upon metalation is predominantly the result of the more efficient nonradiative decay. For both the anionic and the cationic porphyrins the lifetime of the S_1 excited state is about 3 times longer for the free base than for the corresponding

Table 3
Characteristic S_1-fluorescence data of the anionic (A) and cationic (B) metalloporphyrins ($BiTSPP^{3-}$ and $BiTMPyP^{5+}$) and those of the corresponding free-bases (H_2TSPP^{4-} and H_2TMPyP^{4+}).[a]

Species:	H_2TSPP^{4-} [b]			$BiTSPP^{3-}$			H_2TMPyP^{4+}			$BiTMPyP^{5+}$		
Transition:	$S_1(0,0)$	$S_1(0,1)$	$S_1(0,2)$	$S_1(0,0)$	$S_1(0,1)$	$S_1(0,2)$	$S_1(0,0)$	$S_1(0,1)$	$S_1(0,2)$	$S_1(0,0)$	$S_1(0,1)$	$S_1(0,2)$
$\lambda\{S_1(0,i)\}$/nm	647	705	780	609	657	714	658	712	789.375	636	672	730
$I_{max}(0,i)/I_{max}(0,0)$	–	0.712	0.0527	–	0.945	0.0769	–	1.66	0.317	–	0.862	0.1446
$\omega_{1/2}\{S_1(0,i)\}/cm^{-1}$	828	1065	1005	874	925	1070	1021	1342	1373	1042	1091	1065
$\phi\{S_1(0,i)\}/10^{-2}$	3.81	3.49	0.243	0.924	0.924	0.087	0.818	1.78	0.347	0.936	0.845	0.139
$\nu\{S_1(0,i)\}/cm^{-1}$	–	1197	1342	–	1197	1206	–	1151	1370	–	1042	1013
S_1-Stokes/cm^{-1}		360			376			398			651	
S_1-shift (metalation)/cm^{-1}		–			941			–			534	
S_1-shift (substitution)/cm^{-1}		–			–			−279			−685	
$\phi(S_1)/10^{-2}$		7.53 (6.24[c])			1.94			2.95 (2.30[c])			1.92	
$\Phi(S_1\text{-B})/10^{-2}$		5.62			1.34			2.03			1.47	
ϕ(IC)		0.746 (0.828[c])			0.690			0.687 (0.779[c])			0.767	
$\tau(S_1)$/ns		10.03			3.18			5.20			1.38	
$k_r(S_1)/10^6\ s^{-1}$		7.51			6.09			5.68			13.9	
$k_{nr}(S_1)/10^7\ s^{-1}$		9.22			30.8			18.7			71.2	
k_r(Strickler–Berg)/$10^6\ s^{-1}$		8.15			32.4			8.63			34.2	

[a] $\Phi(S_1\text{–B}) = \varphi(\text{IC } S_2 \rightarrow S_1) \times \varphi(S_1)$ and $k_r(S_1) = \varphi(S_1)/\tau(S_1)$.
[b] From Ref. [53]
[c] From Q_y-state.

metalloporphyrin (10 ns vs. 3.2 ns and 5.2 ns vs. 1.4 ns, respectively). The nonradiative decay is about 3.5–4 times faster for the metalloporphyrins than for the corresponding free bases. In spite of the similar factors in the change of the lifetime and the rate constant of the nonradiative decay for both types of porphyrins upon metalation, the decrease of the quantum yield is about 0.26 times for the anionic, while 0.65 times for the cationic porphyrins. This effect may be attributed to the much weaker interaction (i.e., coordination bond) between the metal center and the positively charged ligand of lower Lewis-basicity. However, if the quantum yield decreases only to 65%, but the lifetime to 26% for the cationic complex, then the fluorescence rate constants must increase: to 246%; in contrast with the anionic porphyrin, in which k_{rS_1} slightly decreases (to 81%). These radiative rate constants were also estimated with the Strickler–Berg equation [72]. The values obtained in this way reasonably agree with those derived from the lifetime and quantum yield data for the free bases, but they are significantly higher for the metalloporphyrins (Table 3). Apparently, the equation is not really able to calculate with the effect of the nonradiative decay's significant increase, therefore its measure may be involved in the calculated radiative rate constant.

In the case of arylated porphyrins the fluorescence from the S_1-state shows a relatively rare peculiarity: its spectrum is antisymmetric with respect to that of the absorption [73]. This phenomenon may be accounted for the extension of delocalization by the twisting of aryl substituents to closer to the porphyrin plane, causing an alternating excited state [74]. For distorted porphyrins such as $HgTSPP^{4-}$ and $CdTSPP^{4-}$ smaller fluorescence vs. absorption spectral antisymmetry was observed [58,63]. This feature may be attributed to a smaller magnitude of such structural change because in these cases the dihedral angle of the meso-aryl groups is smaller already in the ground-state than in planar porphyrins. Similar tendencies can be observed for the bismuth(III) porphyrins in our study.

From Table 3, for H_2TSPP^{4-} $I_{max}(0,1)/I_{max}(0,0)$ is 0.71 in fluorescence, while it would be 0.6 if the spectrum were totally antisymmetric to the absorption one from Table 2. The same numbers are 1.66 and 0.23, respectively, for H_2TMPyP^{4+}, 0.94 and 0.39 for $BiTSPP^{4-}$, and 0.86 and 0.33 for $BiTMPyP^{5+}$. The data indicate that not even the cationic free base displays such an antisymmetry, maybe due to slight twisting of the pyridine planes.

Beside the relatively strong emission in the range of 600–800 nm, a weak fluorescence was also observed at 400–520 nm upon excitation at the Soret-band for both $BiTSPP^{3-}$ and $BiTMPyP^{5+}$. Fig. 7 displays these emission bands of both bismuth(III) porphyrins compared to those of the corresponding free bases. On the basis of their high energy and very low intensity, these emission bands can be assigned to the $S_0 \leftarrow S_2$ transition. This kind of fluorescence is scarcely detected but it was also seen for the hydrophobic Zn(II)TPP and H_2TPP species (H_2TPP is tetraphenylporphyrin) [75], as well as for water-soluble $Tl(III)TSPP^{3-}$, $Fe(II)TSPP^{4-}$ and H_2TSPP^{4-} [60,62]. It is worth mentioning that Raman scattering may disturb the detection of this weak emission. However, the previous one can be easily

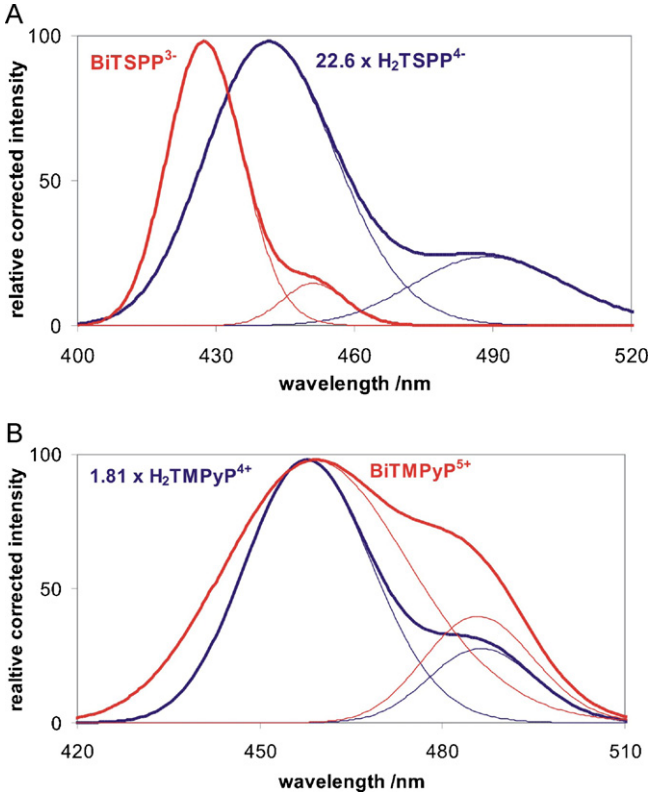

Fig. 7. S_2-fluorescence spectra of the anionic (A) and cationic (B) metalloporphyrins ($BiTSPP^{3-}$ and $BiTMPyP^{5+}$) compared to the corresponding free-bases (H_2TSPP^{4-} and H_2TMPyP^{4+}) upon excitation at the Soret-bands. (Raman scattering has been filtered out.)

Table 4
Characteristic S_2-fluorescence data of the anionic (A) and cationic (B) metalloporphyrins ($BiTSPP^{3-}$ and $BiTMPyP^{5+}$) and those of the corresponding free-bases (H_2TSPP^{4-} and H_2TMPyP^{4+}).

Species:	H_2TSPP^{4-}		$BiTSPP^{3-}$		H_2TMPyP^{4+}		$BiTMPyP^{5+}$	
Transition:	$S_2(0,0)$	$S_2(0,1)$	$S_2(0,0)$	$S_2(0,1)$	$S_2(0,0)$	$S_2(0,1)$	$S_2(0,0)$	$S_2(0,1)$
$\lambda\{S_2(0,i)\}$/nm	441	489	427	451	458	486	459	486
$I_{max}(0,i)/I_{max}(0,0)$	–	0.242	–	0.148	–	0.282	–	0.405
$\omega_{1/2}\{S_2(0,i)\}/cm^{-1}$	1703	1633	1047	793	1173	860	1693	893
$\phi\{S_2(0,i)\}/10^{-5}$	5.09	1.18	71.0	7.97	6.32	1.30	16.4	3.51
$\nu\{S_2(0,i)\}/cm^{-1}$	–	2200	–	1232	–	1285	–	1204
S_2-Stokes/cm^{-1}	1502		308		1824		1118	
S_2–S_1 energy gap/cm^{-1}	7219		6989		6658		5970	
ΔE(B–Q–S_2–S_1 gap)/cm^{-1}	−45		−69		183		467	
S_2-shift (metallation)/cm^{-1}	–		738		–		−60	
S_2-shift (substitution)/cm^{-1}	–		–		−813		−1610	
$\phi(S_2)/10^{-5}$	6.27		79.0		7.62		19.9	
k_r(Strickler–Berg)/10^9 s^{-1}	1.06		1.36		0.879		1.06	
$\tau(S_2)$/fs[a]	(58.9)		(580)		(86.7)		(187)	

[a] Estimated by the Strickler–Berg-equation.

distinguished because its wavelength changes with that of the excitation. The characteristic data for the S_2-fluorescence of the metalloporphyrins studied and those of the corresponding free bases are summarized in Table 4.

The quantum yields of the emission from the S_2 excited state are extremely low (in the range of 10^{-5}–10^{-4}), two orders of magnitude lower than those for the $S_0 \leftarrow S_1$ fluorescence. These values are in good accordance with that determined for H_2TPP ($\Phi_{S_2} = 8.25 \times 10^{-4}$ [75]). These small quantum yields can be, at least partly, attributed to the very short lifetime of the S_2 excited state. Since our TCSPC system was capable for measuring lifetimes as low as about 100 ps, the Strickler–Berg equation [72] was applied for estimation of τ_{S_2}. As the values of τ_{S_2} of in Table 4 indicate they are several hundreds of fs, in accordance with the very low quantum yields.

While in the case of $BiTSPP^{3-}$ an appreciable blue shift of the S_2 emission bands can be observed, compared to those of the corresponding free-base porphyrin, metalation of H_2TMPyP^{4+} hardly changes the energy of these bands. A similar phenomenon is manifested in the values of the S_2-Stokes-shifts (Table 4); coordination of the bismuth(III) ion to the anionic porphyrin dramatically diminishes the Stokes-shift from 1502 cm^{-1} to 308 cm^{-1}, whereas in the case of the cationic porphyrin it results a change from 1824 cm^{-1} to 1118 cm^{-1} (Fig. S2). This phenomenon indicates that metalation of H_2TSPP^{4-} increases the rigidity of the porphyrin ring, decreasing the structural change between ground state and the S_2 excited state. For the cationic system this effect is less pronounced, probably due to the weaker coordination bond as a consquence of the lower Lewis-basicity of the porphyrin ligand. This interpretation is confirmed by the relation of the fluorescence quantum yields. Metalation of the free-base porphyrins significantly increases the values of Φ_{S_2}, as a consequence of the increased rigidity. In the case of the anionic porphyrins the enhancement is about one order of magnitude ($6.25 \times 10^{-5} \rightarrow 7.9 \times 10^{-4}$), while for $BiTMPyP^{5+}$ the corresponding values are only ~2.5 times higher than those of the free base ($7.62 \times 10^{-5} \rightarrow 1.99 \times 10^{-4}$).

The intermediates did not show any fluorescence, neither upon excitation at the Soret- nor at the Q-bands. This observation indicates that their structure is highly distorted, too, as it is also suggested by the large red shift of their Soret-band, hence their excited states decays via efficient IC and, possibly, ISC, as well as photochemical reactions.

3.3. Primary photochemistry

The normal (in-plane) metalloporphyrins do not undergo efficient photoinduced ligand-to-metal charge-transfer reactions as a consequence of their kinetically stable, planar structure. The OOP complexes, however, display a typical photoredox chemistry characterized by irreversible photodegradation of the porphyrin ligand [20,58,59,62,63]. This photochemical behavior is caused by the efficient separation of the reduced metal center and the oxidized macrocycle following the LMCT reaction, which finally leads to irreversible ring cleavage of the ligand, giving open-chain dioxotetrapyrrol derivatives, bilindions. The irradiations were carried out at both the Soret- and the Q-bands, in aerated as well as argon-saturated systems. As Fig. 8 displays, the photoredox degradation of the ligand is accompanied by a less efficient dissociation to the free base and the bismuth(III) ion. The quantum yields obtained for the photochemical reactions of the porphyrins in this work are summarized in Table 5.

In accordance with our earlier observations [20,57,58,63,69], the free-base porphyrins do not show any measurable change upon irradiation at the Q-bands, and only very slight degradation at the Soret-band excitation in both air-saturated and deaerated solutions.

Irradiation of $BiTSPP^{3-}$ at the Soret-band results in the decrease of the absorption at the characteristic bands, indicating an irreversible degradation of the complex, the quantum yield of which is two orders of magnitude higher than that of the free base in the aerated system. This phenomenon, similarly to other 1:1 OOP complexes [57,60,63], indicates that the metal center of relatively large ionic radius promotes the photoinduced LMCT followed by an efficient charge separation.

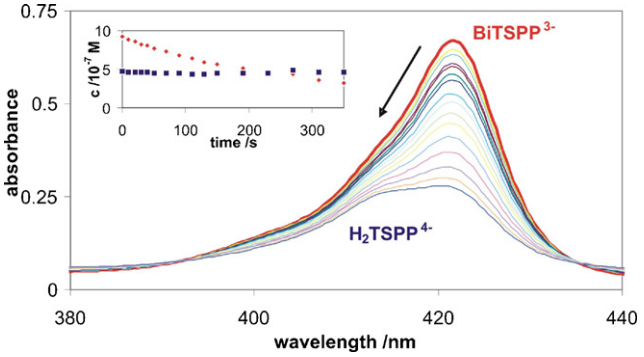

Fig. 8. Spectral changes during the Soret-band irradiation of the anionic final complex formed in the reaction of 1.03×10^{-6} M H_2TSPP^{4-} and 1.00×10^{-4} M Bi^{3+} in the presence of 1 M acetate buffer in deoxygenated solution (pH ≈ 6, I_0(421 nm) = 1.44×10^{-5} M photon/s, l = 1 cm). Insert: concentration vs. time plots for the complex ($BiTSPP^{3-}$, ◆) and the free base released (H_2TSPP^{4-}, ■).

Table 5
The photochemical quantum yields of the free-base and bismuth(III) porphyrins in air-saturated and deoxygenated solution.[a]

Species	H_2TSPP^{4-}	$BiTSPP^{3-}$	i-$BiTSPP^{3-}$	H_2TMPyP^{4+}	$BiTMPyP^{5+}$	i-$BiTMPyP^{5+}$
$\Phi(B)/10^{-5}$	0.60	35.1	2290[b]	6.9	11.2	932
% dissocation	–	5%	99%[b]	–	4%	100%
$\Phi(B\text{–}Ar)/10^{-5}$	0.33	31.0		0.64	2.8	1445
% dissocation	–	6%		–	7%	100%
$\Phi(Q)/10^{-5}$	–	63.0		–	2.2	94.8
% dissocation	–	–		–	–	96%
$\Phi(Q\text{–}Ar)/10^{-5}$	–	59.3		–	1.4	121
% dissocation	–	–		–	–	93%

[a] $\Phi(B)$ and $\Phi(Q)$ are the overall photochemical quantum yields observed in Soret- and Q-band photolysis, and "% dissociation" denotes the photoinduced dissociation of the metal center fraction of the overall quantum yield.
[b] These data are strong estimations on the basis of the small partial molar fraction of i-$BiTSPP^{3-}$ in the solution.

Photoinduced degradation at Soret-band irradiation of H_2TMPyP^{4+} is one order of magnitude more efficient than that of H_2TSPP^{4-} because of the higher efficiency of the cationic porphyrin to form singlet oxygen. After deoxygenation, the photochemical quantum yields of both free-base porphyrins are similarly large. However, deviating from the anionic metalloporphyrin, the quantum yield for the photoinduced degradation of $BiTMPyP^{5+}$ is less than 2 times higher than those for the photolysis of free bases at the Soret-bands. This phenomenon can be interpreted by the lower Lewis-basicity of the cationic ligand, diminishing the efficiency of the LMCT process.

Besides the LMCT process, dissociation of the final complexes (to the free base and the metal center) was also observed, but with a small fraction (about 4–7%) of the overall quantum yield. Irradiation of these bismuth(III) porphyrins at the Q-bands resulted exclusively in redox degradation, although with (about 2 times) higher quantum yields than those observed for Soret-band excitation. This phenomenon suggests that the S_2 excited state of these complexes undergoes more efficient energy dissipation processes than their S_1 excited state does, and following the internal conversion the photoredox process finally originates from this latter one. The absence of oxygen hardly affected the overall quantum yields for the reactions of the anionic final at both Soret- and Q-band irradiations, indicating that dissolved O_2 does not efficently react with the excited-state porphyrins in these systems, probably due to the short lifetimes. Similar tendencies were observed for the photoinduced behavior of the corresponding OOP complex of mercury(II) and cadmium(II) [58,63]. In the case of the cationic complex, the effect of deoxygenation originates from the above-mentioned higher efficiency for the sensitization of oxygen to change its spin multiplicity.

As indicated in Section 3.1, the intermediate state of the cationic bismuth(III) porphyrin could be kept for several hours, thus, its photolysis was also carried out. Deviating from the photochemical behavior of the final OOP complexes, in the case of this intermediate, upon Soret-band irradiation the degradation of the ligand was insignificant (only the ~0.1% of the overall photochemical quantum yield), while upon Q-band irradiation this reaction represented already 4–7% of the whole process. No acceleration of the formation of the final complex was observed upon irradiation. Instead, an efficient dissociation to the free-base porphyrin and the metal ion took place as shown in Fig. 9. The decrease of the Soret-band absorption of the intermediate at 468 nm was accompanied by the simultaneous increase of the corresponding absorption of the free base at 422 nm. This phenomenon indicates that in the intermediate the metal–ligand bond is much weaker than in the final complex, hence excitation promotes the break of this bond rather than an LMCT process. Of course, the transformation to the final complex, as a thermal reaction, could also be observed (Fig. 9).

For a quantitative evaluation of the spectral change both the photoinduced and the dark reactions were taken into consideration. Using the molar absorption spectra of the free base, the intermediate, and the final complex, the actual concentration of each of these species could be determined from the overall spectra of the solution recorded after different periods of irradiation. The evaluation of these data confirmed that, as mentioned above, dissociation was the only photoinduced reaction that appreciably affected the concentration change of the intermediate. Its simultaneous formation from the free base and Bi^{3+} and transformation to the final complex, as thermal reactions, were taken into account. The quantum yield determined in this way for the photoinduced dissociation ($\Phi = 9.4 \times 10^{-3}$) is about two orders of magnitude higher than that for the photoredox degradation of the final complex. A similar value was obtained for the photoinduced dissociation of the axial hydroxo ligand from the anionic cadmium(II) porphyrin and its brominated derivative [63]. This suggests that the coordination bond between the Bi^{3+} ion and the cationic porphyrin is similarly weak as that between the axial hydroxo ligand and the Cd^{2+} center. In the case of the shorter-lived anionic intermediate just an estimation of the quantum yield for the dissociation could be made, its order of magnitude is in accordance with that for the anionic complex, confirming the interpretation above.

Q-band irradiation also led to the dissociation of the cationic intermediate, but with one order of magnitude lower efficiency than that for the Soret-band excitation. This phenomenon can be attributed to the significantly lower energy of the Q-bands. Thus, a slight degradation can compete with the dissociation in this case.

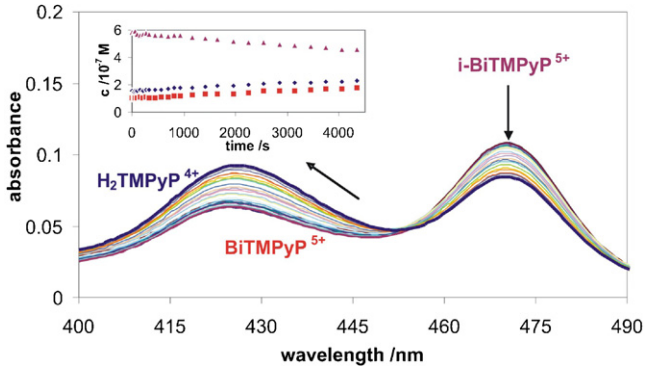

Fig. 9. Spectral changes during the Soret-band irradiation of the cationic intermediate formed in the reaction of 8.43×10^{-7} M H_2TMPyP^{4+} and 2.99×10^{-4} M Bi^{3+} in the presence of 0.01 M acetate buffer in air-saturated solution (pH ≈ 4 $I_0(470\,nm) = 2.88 \times 10^{-7}$ M photon/s, $l = 1$ cm). Insert: concentration vs. time plots for the intermediate (i-$BiTMPyP^{5+}$, ▲), the released free base (H_2TMPyP^{4+}, ◆), and the formed final complex ($BiTMPyP^{5+}$, ■).

Deoxygenation significantly increased the quantum yield at both the Soret- and the Q-band irradiation. This observation may be accounted for the quenching effect of the dissolved oxygen. This suggests that a longer-lived triplet state may also play role in the dissociation process.

3.4. Electronic structure calculations

The main purpose of our electronic structure calculations is to reveal the geometrical structure of the 1:1 bismuth(III) porphyrins (without any axial ligand (BiP), with chloride (Cl–BiP), hydroxide (HO–BiP) or acetate (Ac–BiP) in axial position). The data obtained are compared to those of the free-base porphyrin and its deprotonated form determined earlier [58,59], in order to detect whether there is a correlation between the features of geometry, the electronic spectrum and the photochemical behavior. In the calculations we used a model in which the sulfonato-phenyl or the methyl-pyridinium substituents of the porphyrin ligand, present in our experiments, were omitted. We expect that the out-of-plane distortion of the ligand, influenced mainly by the interaction and relative size of the cavity and the metal ion, can be correctly described with this model. In the case of the corresponding mercury(II) complexes, exploratory calculations with the tetraphenyl-porphyrin ligand indicate that the structure and spectra of HgTPP do not significantly differ from those of HgP [58]. Perspective representation of the calculated geometry of BiP is shown in Fig. 10.

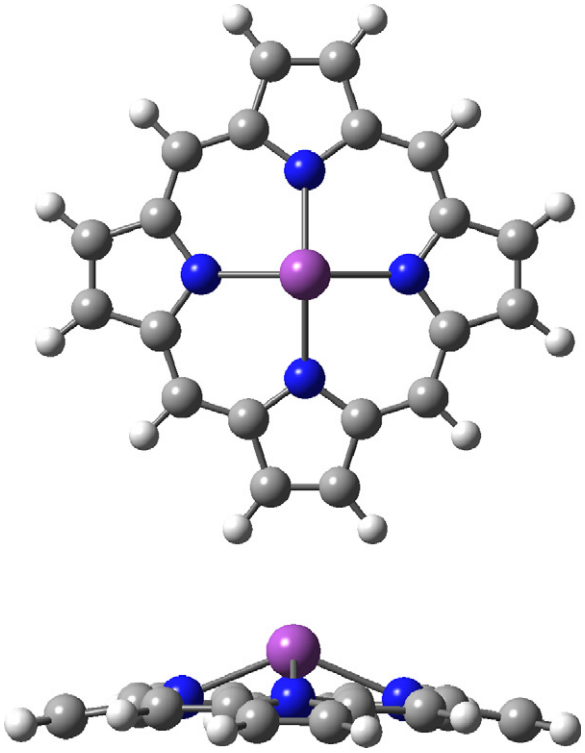

Fig. 10. The structure of the 1:1 bismuth(III) porphin calculated at the B3LYP/LANL2DZ level of theory (side- and top views).

The insertion of the Bi^{3+} ion into the porphyrin causes a significant distortion of the macrocycle. Listed in Table 6 are the calculated geometrical parameters related to the size of the cavity and the geometrical distortion of the macrocycle obtained for the ligand (and its deprotonated form) and the 1:1 bismuth(III) porphyrins. The parameters presented are: d(N–N), the distance between diagonally located N atoms, i.e. the size of the cavity; d_{OOP}, the distance between the metal ion and the plane of the four N atoms (designated as N_4-plane), which is a measure of the magnitude of protrusion of the Bi^{3+} ion from the ligand; d_{dome}, domedness, which we defined as the distance between the plane of the four N atoms and that of the β carbon atoms, which characterizes the magnitude of the distortion of the macrocycle [58]. This last measure of distortion is closely related to the doming angle proposed by Ricciardi et al. [76] for the same purpose (distortion angle). In the case of Cl–BiP, HO–BiP, and Ac–BiP the distance of the metal center and the axial ligand is also given (d(M-axial)).

The B3LYP/LANL2DZ calculations reproduced the D_{2h} structure as the most stable structure of free-base porphyrin, and, in agreement with the expectation, D_{4h} symmetry for the deprotonated species (P^{2-}) [58,59]. The fourfold symmetry is inherited by the BiP complex. As expected, in bismuth(III) porphyrins the metal ion protrudes from the plane of the ligand the magnitude of which depends on the composition. The appealing explanation for this is that the diameter of Bi^{3+} (206 pm) is too large to fit coplanar into the cavity of the porphyrin ring. In the BiP complex the distance of Bi^{3+} from the N atoms is 226 pm, which bond length in a planar arrangement would push apart the N atoms to almost 452 pm, from the 420 pm characterizing the deprotonated porphyrin. However, on the contrary, due to the lifting the Bi^{3+} ion out of the plane of the N atoms the high strain is released so that the diagonal N–N distance can be as small as 416 pm, which is even shorter than that for P^{2-}. At the same time, the Bi^{3+} ion and the four N atoms form a pyramid, which induces the distortion of the plane of C_α carbon tier and through it the rest of the macrocycle. The protrusion of the metal center from the N_4-plane is 88 pm. These results are similar to those obtained for the HgP complex [58], but, interestingly, in that case, d_{OOP} was only 55 pm, and, accordingly, the diagonal N–N distance was 436 pm, although the radius of Hg^{2+} (102 pm) is about the same as that of Bi^{3+} (103 pm). This phenomenon indicates that Hg^{2+}, probably due to its empty s orbital, has a stronger interaction with the porphyrin ligand, leading to a deeper insertion

Table 6
Calculated structural data of the unsubstituted free base (H_2P), its deprotonated form (P^{2-}) and the bismuth(III) porphin without and with potential axial ligands.[a]

Species	H_2P	P^{2-}	BiP^+	(Cl)BiP	(Ac)BiP	(HO)BiP
Symmetry	D_{2h}	D_{4h}	C_{4v}	C_1[b]	C_1[b]	C_1[b]
d(Bi–N)/pm	102[c]	–	226	234	235	239
d(N–N)/pm	407, 425	420	416	419	418	419
d(OOP)/pm	–	–	88	104	108	116
d(dome)/pm	–	–	38	37	40	39
d(M-axial)/pm	–	–	–	274	253	210
$\delta(N–C_\alpha–C_m–C_\alpha)$/°	0	0	6.23	6.59	6.81	6.97

[a] d(N–N) is the distance between diagonally located pyrrol-nitrogens, i.e., the size of cavity; d(OOP) is the distance of the metal center from the coordination cavity; d(dome) is the domedness, i.e., the measure of dome distorsion: the distance between the plane of the pyrrol-nitrogens and that of the β-carbon atoms; the $\delta(N–C_\alpha–C_m–C_\alpha)$ dihedral angle is another measure of the distortion.
[b] This C_1 symmetry is very close to C_s because the orientation of the axial ligands is not totally perpendicular to the plane of pyrrol-nitrogens.
[c] d(H–N).

Table 7
Calculated absorption data of the unsubstituted free base (H_2P), its deprotonated form (P^{2-}) and the bismuth(III) porphin.

Species	H_2P		P^{2-}	BiP^+
Transition-symmetry:	$y = B_{2u}$	$x = B_{1u}$	E_U	E
λ(B)/nm	357	378	390	394
f(B)	0.579	0.356	1.33	0.741
B-shift/cm^{-1}	–	–	−1551	−1836
λ(Q)/nm	511	553	606	540
f(Q)	0.00030	0.00240	0.0492	0.00320
Q-shift/cm^{-1}	–	–	−2296	−286

The shifts were calculated from the average of *y* and *x* transitions of the free-base porphin; *f* is the oscillator strength.

into the cavity of the ligand, moderately pushing apart the N atoms. The 88-pm out-of-plane distance for BiP is in accordance with that obtained for a bismuth(III) corrole (105 pm) also by DFT calculation [43] because the corrole ring is one methylidine bridge smaller than the porphin ring.

The macrocycle distortion from the planar structure is characterized by d_{dome} values of about 38 pm for the bismuth(III) porphyrins, similarly to the HgP complex (40 pm [58]). Apparently the axial ligands do not appeciably influence this value, although they significantly enhance the out-of-plane distance (104 pm with Cl^-, 108 pm with Ac^-, and 116 pm with HO^-), in accordance with our earlier results regarding the water-soluble cadmium(II) porphyrins [63], and with the solid state structures of hydrophobic bismuth(III) porphyrins [24,26,30,31,36]. In our calculations on other typical 1:1 out-of-plane complexes we obtained very similar domedness [20,58,59]. As the spectral, photophysical and photochemical properties of several OOP porphyrins are very similar, it would be reasonable to assume that the common property, the doming is the source of the common properties.

We also calculated electronic spectra, using the TD-DFT method, for a better understanding the role of the macrocycle distortion (Table 7). The band assignment can be performed based on the observation that the energy of the $\pi\pi^*$ transitions of ^1E_u symmetry in D_{4h} structures increases in the series: (1) Q-, (2) B- or Soret-, (3) N-, (4) L- and (5) M-band [77]. The symmetry of transitions can change if the geometry of the molecule is distorted [78]. The Soret- and the Q-bands, according to our calculations (in agreement with the literature, see e.g. refs. [76,79], and our earlier experiences [58,63]) were not found to be pure one-electron excitations but mixtures of them, often with several one-electron excitations between molecular orbitals outside from the frontier 4 MO-models [80] superposed with comparable weight, mainly at the Soret-bands (Tables S1–S3). Also the results of calculation indicate the reduced symmetry (D_{2h}) in free-base porphyrin due to the effect of the diagonally located H atoms on the pyrrolic nitrogens. Hence both the Soret- and the Q-bands split as seen in Table 7, although experimentally the previous is not visible, which suggests that the S_2-state is non-degenerate. Nevertheless, it is worth mentioning that the wavelengths obtained by B3LYP/LANL2DZ calculations are closer to the experimental ones than those given earlier by M05 calculations [58]. Besides, the Soret-band for the deprotonated free-base (P^{2-}) obtained by our present calculations displays a significant red shift, in accordance with the expectations, while the results of the former (M05) calculations indicated a blue shift. The Q-bands show red shift by both calculations. The red shifts obtained for the deprotonated porphyrin can be interpreted by the increase of aromatization (compared to H_2P with two diagonally placed protonated pyrrols) as a consequence of the same participation of all four pyrrol-nitrogens in the delocalization.

Similarly to the experimentally observed tendency (Tables 1 and 2), for the bismuth(III) porphyrin the calculated bands (both Soret- and Q-) are red-shifted compared to those of the free-base porphyrin, but to a lesser extent than in the case of P^{2-} (Table 7). This suggests, in accordance with our earlier observations [58], that in an out-of-plane complex the electronic properties of macrocycle approach that of P^{2-}. This phenomenon confirms that the distortion of the porphyrin plane is not the only factor responsible for the common spectral behavior of out-of-plane porphyrins.

4. Conclusion

The bismuth(III) ion forms kinetically labile complexes with water-soluble H_2TSPP^{4-} and H_2TMPyP^{4+} porphyrins through intermediate metalloporphyrins. The final complexes display the typical spectral properties and photoinduced behavior of out-of-plane metalloporphyrins in accordance with the quantum chemical calculations regarding the structure and the electronic spectra of these species. The tendencies of the effects of the ligand charge on the photophysical and photochemical properties of these complexes can be interpreted by the different Lewis-basicities of the porphyrins. The spectral and photoinduced features of the intermediates suggest that the metal–ligand coordination bond is weaker in these species than in the corresponding final complexes, and the distortion of porphyrin is probably higher. The shifts of the absorption bands upon metalation indicate that the structural distortion results in stronger perturbation on the S_2- than on the S_1-states of the porphyrin ligand, a phenomenon which is also more pronounced for the intermediate complexes. These results contribute to the exploration and interpretation of the effects of the ionic substituents on the porphyrin ligands in the respect of the photophysical and photochemical behavior of OOP metalloporphyrins. Further studies on the formation and decay kinetics of the intermediate bismuth(III) porphyrin complexes are in progress to elucidate the role of the charge of the ligand and the structure in these processes.

Acknowledgments

This work was supported by the National Development Agency (TÁMOP 4.2.2.-08/1/2008–0018, Livable environment and healthier people – Bioinnovation and Green Technology Research at the University of Pannonia, the project is being co-financed by the European Social Fund with the support of the European Union). The valuable assistance of Gergely Harrach is also acknowledged.

Appendix A. Supplementary data

Supplementary data associated with this article can be found, in the online version, at doi:10.1016/j.jphotochem.2011.10.011.

References

[1] C.K. Mathews, K.E. van Holde, K.G. Ahern, Biochemistry, Addison Wesley Longman, San Francisco, 2000.
[2] R.H. Garrett, C.M. Grisham, Biochemistry, Saunders College Publishing, 1999.

[3] G. Knör, A. Strasser, Enhanced photoreactivity of zirconium(IV) and hafnium(IV) porphyrin complexes promoted by water molecules, Inorg. Chem. Commun. 9 (2005) 471–473.
[4] M.D. Lim, I.M. Lorkovic, P.C. Ford, NO and NO_x interactions with model group 8 metalloporphyrins, J. Inorg. Biochem. 99 (2005) 151–165.
[5] G.G. Martirosyan, A.S. Azizyan, T.S. Kurtikyan, P.C. Ford, Low Temperature NO disproportionation by Mn porphyrin. Spectroscopic characterization of the unstable Nitrosyl Nitrito complex Mn^{III}(TPP)(NO)(ONO), Chem. Commun. (2004) 1488–1489.
[6] A.G. Tovmasyan, N.S. Babayan, L.A. Sahakyan, A.G. Shahkhatuni, G.H. Gasparyan, R.M. Aroutiounian, R.K. Ghazaryarn, Synthesis and in vitro anticancer activity of water-soluble cationic pyridylporphyrins and their metallocomplexes, J. Porphyr. Phthalocya. 12 (2008) 1100–1110.
[7] Q.G. Ren, X.T. Zhou, H.B. Ji, Progress of water-soluble metalloporphyrins in catalytic reactions, Chin. J. Org. Chem. 30 (2010) 1605–1614.
[8] K. Kawamura, S. Igarashi, T. Yotsuyanagi, Catalytic activity of noble metal ions for the degradation of 5, 10,15,20-tetrakis(4-sulfonatophenyl)porphine in the presence of oxidizing agent, and its application to the determination of ultra trace amounts of ruthenium, Microchim. Acta 172 (2011) 319–326.
[9] E.B. Fleischer, J.H. Wang, The detection of a type of reaction intermediate in the combination of metal ions with porphyrins, J. Am. Chem. Soc. 82 (1960) 3498–3502.
[10] K.M. Barkigia, J. Fajer, A.D. Adler, G.J.B. Williams, Crystal and molecular structure of (5, 10,15,20-tetra-N-propylporphinato)lead(II): a roof porphyrin, Inorg. Chem. 19 (1980) 2057–2061.
[11] M.S. Liao, J.D. Watts, M.J. Huang, DFT/TDDFT study of Lanthanide(III) mono- and bisporphyrin complexes, J. Phys. Chem. A 110 (2006) 13089–13098.
[12] V.E.J. Walker, N. Castillo, C.F. Matta, R.J. Boyd, The effect of multiplicity on the size of Iron(II) and the structure of Iron(II) porphyrins, J. Phys. Chem. A 114 (2010) 10315–10319.
[13] M. Tabata, M. Tanaka, A new method for the determination of the stability constant of metalloporphyrins, use of the catalytic effect of Mercury(II) on metalloporphyrin formation, J. Chem. Soc., Chem. Commun. (1985) 42–43.
[14] M. Tabata, W. Miyata, N. Nahar, Kinetics and mechanism of metal-substitution reaction of homodinuclear mercury(II) porphyrin with zinc(II) with particular reference to a heterodinuclear metalloporphyrin intermediate, Inorg. Chem. 34 (1995) 6492–6496.
[15] C. Grant, P. Hambright, Kinetics of electrophilic substitution reactions involving metal ions in metalloporphyrins, J. Am. Chem. Soc. 91 (1969) 4195–4197.
[16] L.R. Robinson, P. Hambright, Mercury(II) reactions with water-soluble porphyrins, Inorg. Chem. 31 (1992) 652–656.
[17] C. Stinson, P. Hambright, The copper–cadmium N-methyltetraphenylporphyrin electrophilic substitution reaction: evidence for a cis attack, J. Am. Chem. Soc. 99 (1977) 2357.
[18] K.M. Barkigia, M.D. Berber, J. Fajer, C.J. Medforth, M.W. Renner, K.M. Smith, Nonplanar porphyrins. X-ray structures of (2,3,7,8,12,13,17,18-octaethyl- and -octamethyl-5,10,15,20-tetraphenylporphinato)zinc(II), J. Am. Chem. Soc. 112 (1990) 8851–8857.
[19] J.Y. Tung, J.-H. Chen, Crystal and molecular structure of an eight-coodinate *N*-methyltetraphenylporphyrin complex: diacetato(*N*-methyl-*meso*-tetraphenylporphyrinato)thallium(III), Inorg. Chem. 39 (2000) 2120–2124.
[20] O. Horváth, R. Huszánk, Z. Valicsek, G. Lendvay, Photophysics and photochemistry of kinetically labile, water-soluble porphyrin complexes, Coord. Chem. Rev. 250 (2006) 1792–1803.
[21] R.D. Shannon, Revised effective ionic radii and systematic studies of interatomic distances in halides and chalcogenides, Acta Crystallogr. A32 (1976) 751–767.
[22] A. Treibs, Metallkomplexe von porphyrinen, Justus Liebigs Ann. Chem. 728 (1969) 115–143.
[23] J.W. Buchler, K.L. Lay, Arsen-, Antimon- und Wismutkomplexe des Octaäthylporphins (1), Inorg. Nucl. Chem. Lett. 10 (1974) 297–300.
[24] P. Sayer, M. Gouterman, C.R. Connell, Metalloid porphyrins and phthalocyanines, Acc. Chem. Res. 15 (1982) 73–79.
[25] B. Boitrel, M. Breede, P.J. Brothers, M. Hodgson, L. Michaudet, C.E.F. Rickard, N.A. Salim, Bismuth porphyrin complexes: syntheses and structural studies, Dalton Trans. (2003) 1803–1807.
[26] Z. Halime, L. Michaudet, M. Razavet, C. Ruzié, B. Boitrel, Synthesis, characterisation and properties of bismuth(III) ester pendant arm picket porphyrins, Dalton Trans. (2003) 4250–4254.
[27] Z. Halime, M. Lachkar, P. Brossier, B. Boitrel, Influence of pendant arms bearing ligating groups on the structure of bismuth porphyrins: implications for labeling immunoglobulins used in medical applications, Bioconjugate Chem. 15 (2004) 1193–1200.
[28] T. Barbour, W.J. Belcher, P.J. Brothers, C.E.F. Rickard, D.C. Ware, Preparation of group 15 (phosphorous, antimony, and bismuth) complexes of *meso*-tetra-*p*-tolylporphyn (TTP) and X-ray crystal structure of [Sb(TPP)($OCH(CH_3)_2$)$_2$]Cl, Inorg. Chem. 31 (1992) 746–757.
[29] L. Michaudet, D. Fasseur, R. Guilard, Z. Ou, K.M. Kadish, S. Dahaoui, C. Lecomte, Synthesis, characterization and electrochemistry of bismuth porphyrins, X-ray crystal structure of (OEP)Bi(SO_3CF_3), J. Porphyr. Phthalocya. 4 (2000) 261–270.
[30] B. Boitrel, Z. Halime, L. Michaudet, M. Lachkar, L. Toupet, Structural characterization of the first mononuclear bismuth porphyrin, Chem. Commun. (2003) 2670–2671.
[31] L. Michaudet, P. Richard, B. Boitrel, Synthesis and crystal structure of an unprecedented bismuth porphyrin containing ester pendant arms, Chem. Commun. (2000) 1589–1590.
[32] B. Boitrel, Z. Halime, S. Balieu, M. Lachkar, The coordination of bismuth by porphyrins, C. R. Chim. 10 (2007) 583–589.
[33] L. Michaudet, Z. Halime, M. Lachkar, B. Boitrel, Pre-shaped aromatic picket porphyrins bearing neutral oxygen donors and their bismuth complexes: synthesis and coordination studies, Lett. Org. Chem. 3 (2006) 753–758.
[34] S. Balieu, Z. Halime, M. Lachkar, B. Boitrel, Bismuth insertion in functionalized porphyrins: influence of the structure delivering substituted malonic acid groups, J. Porphyr. Phthalocya. 12 (2008) 1223–1231.
[35] S. Balieu, A.M. Bouraiou, B. Carboni, B. Boitrel, Synthesis of a boronic ester-appended bismuth(III) porphyrin as a potential alpha-particle bi-emitter, J. Porphyr. Phthalocya. 12 (2008) 11–18.
[36] Z. Halime, M. Lachkar, T. Roisnel, E. Furet, J.-F. Halet, B. Boitrel, Bismuth and lead hanging-carboxylate porphyrins: an unexpected homobimetallic Lead(II) complex, Angew. Chem. Int. Ed. 46 (2007) 5120–5124.
[37] J. Janczak, Synthesis and characterisation of bismuth(III) phthalocyaninate complex: $[BiPc]_4[Bi_6I_{11}Cl_{11}]$, J. Mol. Struct. 965 (2010) 125–130.
[38] G. Ostendorp, H. Homborg, Darstellung und eigenschaften von diphthalocyaninaten des Bismuts, $[Bi(Pc)_2]^k$ (k = 1–0, 1+); Kristallstruktur von gemischtvalentem $[Bi(Pc)_2]^\bullet$ CH_2Cl_2, Z. Anorg. Allg. Chem. 622 (1996) 873–880.
[39] M. Gouterman, G.H. Wagnière, L.C. Snyder, Spectra of porphyrins: Part II. Four orbital model, J. Mol. Spectrosc. 11 (1963) 108–127.
[40] M. Vitasovic, M. Gouterman, H. Linschitz, Calculations on the origin of hyperporphyrin spectra in sequentially protonated meso-(dimethylaminophenyl) porphyrins, J. Porphyr. Phthalocya. 5 (2001) 191–197.
[41] J.R. Weinkauf, S.W. Cooper, A. Schweiger, C.C. Wamser, Substituent and solvent effects on the hyperporphyrin spectra of diprotonated tetraphenylporphyrins, J. Phys. Chem. A 107 (2003) 3486–3496.
[42] G.P. Chacko, P. Hambright, Acid-, anion- and base-catalyzed solvolysis reactions of a water soluble bismuth(III) porphyrin, Inorg. Chem. 33 (1994) 5595–5597.
[43] L.M. Reith, M. Himmelsbach, W. Schoefberger, G. Knör, Electronic spectra and photochemical reactivity of bismuth corrole complexes, J. Photoch. Photobio. A 218 (2011) 247–253.
[44] F.D. 'Souza, G.R. Deviprasad, M.E. Zandler, Aggregation and axial ligation behavior of water soluble, pyrrole-β brominated porphyrins, J. Chem. Soc., Dalton Trans. (1977) 3699–3703.
[45] J.N. Demas, G.A. Crosby, The measurement of photoluminescence quantum yields, J. Phys. Chem. 75 (1971) 991–1024.
[46] J. Van Houten, R.J. Watts, Temperature-dependence of photophysical and photochemical properties of tris(2,2′-bipyridyl)ruthenium(II) ion in aqueous-solution, J. Am. Chem. Soc. 98 (1976) 4853–4858.
[47] J.F. Rabek, Experimental Methods in Photochemistry and Photophysics, Wiley-Interscience Publication/John Wiley & Sons Ltd., New York, 1982.
[48] S.L. Murov, Handbook of Photochemistry, Marcel Dekker, New York, 1973.
[49] A.D. Kirk, C. Namasivayam, Errors in ferrioxalate actinometry, Anal. Chem. 55 (1983) 2428–2429.
[50] A.D. Becke, A new mixing of Hartree–Fock and local density-functional theories, J. Chem. Phys. 98 (1993) 1372–1377.
[51] A.D. Becke, Density-functional thermochemistry. 3. The role of exact exchange, J. Chem. Phys. 98 (1993) 5648–5652.
[52] C. Lee, W. Yang, R.G. Parr, Development of the Colle–Salvetti correlation-energy formula into a functional of the electron density, Phys. Rev. B37 (1988) 785–789.
[53] P.J. Hay, W.R. Wadt, Abinitio effective core potentials for molecular calculations – potentials for transition-metal atoms Sc to Hg, J. Chem. Phys. 82 (1985) 270–283.
[54] W.R. Wadt, P.J. Hay, Abinitio effective core potentials for molecular calculations – potentials for main group elements Na to Bi, J. Chem. Phys. 82 (1985) 284–298.
[55] P.J. Hay, W.R. Wadt, Abinitio effective core potentials for molecular calculations – potentials for K to Au including the outermost core orbitals, J. Chem. Phys. 82 (1985) 299–310.
[56] M.J. Frisch, G.W. Trucks, H.B. Schlegel, G.E. Scuseria, M.A. Robb, J.R. Cheeseman, J.A. Montgomery Jr., T. Vreven, K.N. Kudin, J.C. Burant, J.M. Millam, S.S. Iyengar, J. Tomasi, V. Barone, B. Mennucci, M. Cossi, G. Scalmani, N. Rega, G.A. Petersson, H. Nakatsuji, M. Hada, M. Ehara, K. Toyota, R. Fukuda, J. Hasegawa, M. Ishida, T. Nakajima, Y. Honda, O. Kitao, H. Nakai, M. Klene, X. Li, J.E. Knox, H.P. Hratchian, J.B. Cross, V. Bakken, C. Adamo, J. Jaramillo, R. Gomperts, R.E. Stratmann, O. Yazyev, A.J. Austin, R. Cammi, C. Pomelli, J.W. Ochterski, P.Y. Ayala, K. Morokuma, G.A. Voth, P. Salvador, J.J. Dannenberg, V.G. Zakrzewski, S. Dapprich, A.D. Daniels, M.C. Strain, O. Farkas, D.K. Malick, A.D. Rabuck, K. Raghavachari, J.B. Foresman, J.V. Ortiz, Q. Cui, A.G. Baboul, S. Clifford, J. Cioslowski, B.B. Stefanov, G. Liu, A. Liashenko, P. Piskorz, I. Komaromi, R.L. Martin, D.J. Fox, T. Keith, M.A. Al-Laham, C.Y. Peng, A. Nanayakkara, M. Challacombe, P.M.W. Gill, B. Johnson, W. Chen, M.W. Wong, C. Gonzalez, J.A. Pople, Gaussian 03, Revision E.01, Gaussian, Inc., Wallingford, CT, 2004.
[57] O. Horváth, Z. Valicsek, A. Vogler, Unique photoreactivity of mercury(II) 5,10,15,20-tetrakis(4-sulfonatophenyl)porphyrin, Inorg. Chem. Commun. 7 (2004) 854–857.
[58] Z. Valicsek, G. Lendvay, O. Horváth, Equilibrium, photophysical, photochemical and quantum chemical examination of anionic mercury(II) mono- and bisporphyrins, J. Phys. Chem. B 112 (2008) 14509–14524.
[59] Z. Valicsek, G. Lendvay, O. Horváth, Equilibrium, photophysical, photochemical and quantum chemical examination of anionic mercury(I) porphyrins, J. Porphyr. Phthalocya. 13 (2009) 910–926.
[60] Z. Valicsek, O. Horváth, Formation, photophysics and photochemistry of thallium(III) 5,10,15,20-tetrakis(4-sulphonatophenyl)porphyrin; new supports of typical sitting-atop features, J. Photoch. Photobio. A 186 (2007) 1–7.

[61] R. Huszánk, O. Horváth, A heme-like, water-soluble iron(II) porphyrin: thermal and photoinduced properties, evidences for sitting-atop structure, Chem. Commun. (2005) 224–226.
[62] R. Huszánk, G. Lendvay, O. Horváth, Air stable, heme-like water-soluble iron(II) porphyrin: in-situ preparation and characterization, J. Bioinorg. Chem. 12 (2007) 681–690.
[63] Z. Valicsek, O. Horváth, G. Lendvay, I. Kikaš, I. Škorić, Formation, photophysics, and photochemistry of cadmium(II) complexes with 5,10,15,20-tetrakis(4-sulfonatophenyl)porphyrin and its octabromo derivative: the effects of bromination and the axial hydroxo ligand, J. Photoch. Photobio. A 218 (2011) 143–155.
[64] R.F. Pasternack, N. Sutin, D.H. Turner, Some very rapid reactions of porphyrins in aqueous-solution, J. Am. Chem. Soc. 98 (1976) 1908–1913.
[65] K. Kalyanasundaram, Photochemistry of Polypyridine and Porphyrin Complexes, Academic Press, New York, 1992.
[66] K. Kalyanasundaram, M. Neumann-Spallart, Photophysical and redox properties of water-soluble porphyrins in aqueous media, J. Phys. Chem. 86 (1982) 5163–5169.
[67] J.R. Platt, Classification and assignments of ultraviolet spectra of conjugated organic molecules, J. Opt. Soc., Am. 43 (1953) 252–256.
[68] M. Gouterman, Study of the effects of substitution on the absorption spectra of porphyrin, J. Chem. Phys. 30 (1959) 1139–1161.
[69] Z. Valicsek, O. Horváth, K.L. Stevenson, Photophysics and photochemistry of water-soluble, sitting-atop bis-thallium(I) 5,10,15,20-tetrakis(4-sulfonatophenyl)porphyrin, Photochem. Photobiol. Sci. 3 (2004) 669–673.
[70] J.A. Shelnutt, X.-Z. Song, J.-G. Ma, S.-L. Jia, W. Jentzen, C.J. Medforth, Nonplanar porphyrins and their significance in proteins, Chem. Soc. Rev. 27 (1998) 31–41.
[71] J.A. Shelnutt, Normal-coordinate structural decomposition and the vibronic spectra of porphyrins, J. Porphyr. Phthalocya. 5 (2001) 300–311.
[72] S.J. Strickler, R.A. Berg, Relationship between absorption intensity and fluorescence lifetime of molecules, J. Chem. Phys. 37 (1962) 814–822.
[73] M. Gouterman, L. Stryer, Fluorescence polarization of some porphyrins, J. Chem. Phys. 37 (1962) 2260–2266.
[74] H.N. Fonda, J.V. Gilbert, R.A. Cormier, J.R. Sprague, K. Kamioka, J.S. Connolly, Spectroscopic, photophysical, and redox properties of some meso-substitued free-base porphyrins, J. Phys. Chem. 97 (1993) 7024–7033.
[75] H.Z. Yu, J.S. Baskin, A.H. Zewail, Ultrafast dynamics of porphyrins in the condensed phase. II. Zinc tetraphenylporphyrin, J. Phys. Chem. A 106 (2002) 9845–9854.
[76] G. Ricciardi, A. Rosa, E.J. Baerends, S.J.A. van Gisbergen, Electronic structure, chemical bond, and optical spectra of metal bis(porphyrin) complexes: a DFT/TDDFT study of the bis(porphyrin)M(IV) (M = Zr, Ce, Th) series, J. Am. Chem. Soc. 124 (2002) 12319–12334.
[77] A.D. Adler, F.R. Longo, F.V. Varadi, Preparation of metalloporphyrins, Inorg. Synth. 16 (1976) 213–220.
[78] H. Baker, P. Hambright, L. Wagner, Metal ion porphyrin interactions. II. Evidence for the nonexistence of sitting atop complexes in aqueous solution, J. Am. Chem. Soc. 95 (1973) 5942–5946.
[79] I. Mayer, Bond order and valence indices: a personal account, J. Comput. Chem. 28 (2007) 204–221.
[80] M. Gouterman, in: D. Dolphin (Ed.), Porphyrins, vol. 111, Academic Press, New York, 1978, p. 79.